

A Comparative Study of Car-Trailer Dynamics Models

Yuping He and Jing Ren
Univ of Ontario Institute of Technology

ABSTRACT

The paper examines typical vehicle dynamics models used for the design of car-trailer active safety systems, including active trailer braking and steering. A linear 3 degree-of-freedom (DOF), a nonlinear 4 DOF and a nonlinear 6 DOF car-trailer model are generated. Then, these models are compared with a car-trailer model developed with the commercial software package, CarSim. The benchmark investigation of the car-trailer models is carried out through examining numerical simulation results obtained in two emulated tests, i.e., a single lane-change and a Fishhook maneuver. In the vehicle modeling, a mathematical model of a tire with flexible sidewalls is included to account for transient tire forces. Steady-state aerodynamic forces are included in these models. The deviation of the model dynamic responses, e.g., the variation of the articulation angle between the car and trailer, is discussed. With the benchmark investigation, the car-trailer models in terms of fidelity, complexity, and applicability for active safety system design are addressed.

CITATION: He, Y. and Ren, J., "A Comparative Study of Car-Trailer Dynamics Models," *SAE Int. J. Passeng. Cars - Mech. Syst.* 6(1):2013, doi:10.4271/2013-01-0695.

INTRODUCTION

A car-trailer system consists of a towing unit, e.g., a car, and a towed unit, i.e., a trailer. The car and trailer are connected at an articulated point by a hitch [1]. With respect to single-unit cars, car-trailer systems may exhibit poor lateral stability at high speeds because of their double-unit structure. For these vehicles, three unique unstable motion modes have been identified, including the trailer swing (oscillatory instability), jack-knifing, and rollover. These unstable motion modes are the common causes for fatal accidents occurring on highways [2]. For a car-trailer system, it is difficult for the driver to sense the trailer motions, as the driver's perception is based mainly on the car response, rather than the trailer. The articulation joint and the car suspension isolate the driver from trailer motions. The unstable motion modes of trailer swing, jack-knifing, and/or rollover are usually directly related to the trailer response. Moreover, most drivers of these articulated vehicles are non-professional driver, whose inexperience may make them susceptible to experiencing instabilities [2]. To date, the majority of car-trailer systems use passive mechanisms to enhance the lateral stability at high speeds. Unfortunately, the high-speed lateral stability of a car-trailer system cannot be guaranteed with a passive mechanism, because the operation conditions vary significantly, e.g., the variation of payload, location of payload, and center of gravity (CG) of the trailer [3].

To address the safety problem of car-trailer systems, various active safety systems have been proposed, which include active trailer steering and active trailer braking [2]. To develop an effective car-trailer active safety system, it is critical to design a robust control algorithm that prevents the unstable motion modes. In the initial development phase of road vehicle active safety systems, various vehicle models have been used to derive the corresponding control algorithms. In the controller design for articulated vehicle active safety systems, different vehicle models with various degrees of freedom (DOF) have been used [2, 4, 5]. However, the applicability of various articulated vehicle models for active safety systems design has not been addressed.

This paper will tackle this problem. Through the benchmark investigation, four car-trailer models are examined in terms of fidelity, complexity, and applicability for active safety system design. The comparison study of the car-trailer models is implemented through investigating numerical simulation results obtained in two emulated tests, i.e., a single lane-change and a Fishhook maneuver. The deviations of the model dynamic responses are discussed.

The rest of the paper is organized as follows: Section 2 introduces the four car-trailer models; the vehicle models are compared and analyzed in Section 4; finally, conclusions are drawn in Section 5.

VEHICLE SYSTEM MODELS

This section introduces the following four car-trailer models: 1) a linear yaw/plane model with 3 DOF; 2) a nonlinear yaw/plane model with 4 DOF; 3) a nonlinear yaw/roll model with 6 DOF; and 4) a nonlinear CarSim model with 21 DOF [6].

Linear Yaw/Plane Model with 3 DOF

Figure 1 shows a yaw/plane model with 4 DOF. For this model, the motions considered include: 1) the longitudinal motion of the car at velocity U at the car's CG; 2) the lateral motion of the car at velocity V ; 3) the yawing motion of the car at yaw rate $\dot{\Psi}_1$; and 4) the articulation angle ψ_2 between the car and trailer. As shown in Figure 1, the system is telescoped laterally and each axle set is represented by one wheel. In this model, aerodynamic forces, rolling and pitching motions are ignored. From Newton's law of dynamics, the equations of motion for the car are [7]:

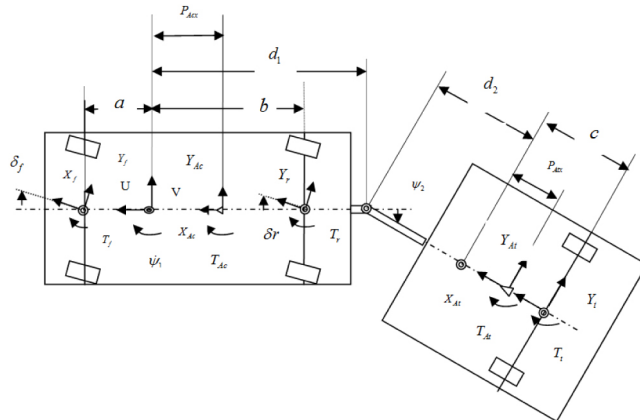


Figure 1. Schematic representation of the yaw plane model

$$m_c \cdot (\dot{U} - V \cdot \dot{\Psi}_1) = -X_f \cdot \cos \delta_f - X_r + X_{\psi_2} \quad (1)$$

$$m_c \cdot (\dot{V} + U \cdot \dot{\Psi}_1) = Y_f + Y_r + X_f \cdot \sin \delta_f - Y_{\psi_2} \quad (2)$$

$$I_c \cdot \ddot{\Psi}_1 = a \cdot Y_f - b \cdot Y_r + a \cdot X_f \cdot \sin \delta_f + d_1 \cdot Y_{\psi_2} \quad (3)$$

and the equations of motion for the trailer are [7]:

$$m_t \cdot (\dot{U}_t - V_t \cdot \dot{\Psi}_t) = -X_t - Y_{\psi_2} \cdot \sin \Psi_2 - X_{\psi_2} \cdot \cos \Psi_2 \quad (4)$$

$$m_t \cdot (\dot{V}_t + U_t \cdot \dot{\Psi}_t) = Y_t + Y_{\psi_2} \cdot \cos \Psi_2 - X_{\psi_2} \cdot \sin \Psi_2 \quad (5)$$

$$I_t \cdot \ddot{\Psi}_t = c \cdot Y_f - d_2 \cdot (X_{\psi_2} \cdot \sin \Psi_2 - Y_{\psi_2} \cdot \cos \Psi_2) \quad (6)$$

where Y_f , Y_r and Y_t are the lateral force on the car front tire, the lateral force on the car rear tire, and the lateral force on the trailer tire, respectively. The velocities at the articulation joint described in either the car-body fixed coordinate system or the trailer-body fixed coordinate system should be compatible. Expressing all the variables in car-body fixed coordinate system will reduce the above six equations to a set of four equations. The reader is referred to [7] for the transition of equations. The resulting four equations describe the general motion of a car-trailer system that may be accelerating or braking.

A linear tire model is used and it may be expressed by the following equations [8].

$$Y_f = C_f \cdot \alpha_f \quad (7)$$

$$Y_r = C_r \cdot \alpha_r \quad (8)$$

$$Y_t = C_t \cdot \alpha_t \quad (9)$$

where C_f , C_r and C_t are the tire cornering stiffness, α_f , α_r and α_t are the side-slip angles of the tires. The side-slip angles are given by [7]:

$$\alpha_f = \frac{V + a \cdot \dot{\Psi}_1}{U} - \delta_f \quad (10)$$

$$\alpha_r = \frac{V - b \cdot \dot{\Psi}_1}{U} \quad (11)$$

$$\alpha_t = \Psi_2 - \frac{V - (d_1 + d_2 + c) \cdot \dot{\Psi}_1 + (d_2 + c) \cdot \dot{\Psi}_2}{U} \quad (12)$$

To derive the linear governing equations of motion of the car-trailer model, it is assumed that: the car forward speed U is constant; lateral tire forces, Y_f , Y_r and Y_t , are the only external forces; articulated angle ψ_2 is small, so that $\cos \psi_2 = 1$, $\sin \psi_2 = 0$; products of V , $\dot{\Psi}_1$ and ψ_2 are small enough to ignore. With the above assumptions, only three motions are considered in the resulting model: 1) the lateral motion of the car at velocity V ; 2) the yawing motion of the car at yaw rate $\dot{\Psi}_1$; and 3) the articulation angle ψ_2 between the car and trailer. The resulting model is a linear yaw/plane model with 3 DOF (hereafter called 3DOF-L). The linear yaw/plane model can be expressed in the state space as

$$M \{ \dot{X} \} + D \{ X \} + F \delta_f = 0 \quad (13)$$

where the state variable vector is defined as

$$\{X\} = \{V \ \dot{\Psi}_1 \ \dot{\Psi}_2 \ \dot{\Psi}_2\} \quad (14)$$

The matrices M, D and F are listed in [Appendix A](#). [Table 1](#) lists the notations and the primary parameters of the car-trailer system.

Table 1. The primary parameters of the car-trailer system

Car mass	m_c	2000 kg
Car yaw inertia	I_c	3000 kgm ²
Car dimension	a	1.5 m
Car dimension	b	1.7 m
Car dimension	d_l	2.8m
Trailer mass	m_t	2300 kg
Trailer yaw inertia	I_t	3900 kgm ²
Trailer dimension	c	5 m
Trailer dimension	d_2	0 m
Front tire cornering stiffness (combined)	C_f	-80000 Nm/rad
Rear tire cornering stiffness (combined)	C_r	-80000 Nm/rad
Trailer tire cornering stiffness (combined)	C_t	-60000 Nm/rad

Nonlinear Yaw/Plane Model with 4 DOF

For the nonlinear yaw/plane model with 4 DOF (hereafter called 4DOF-NL), the motions considered include the longitudinal motion of the car and the other three motions that are considered in the 3DOF-L model. The 4DOF-NL model incorporates some effects that are not taken into account in the 3DOF-L model. The tire model used in the 4DOF-NL model is based on the Magic Formula by Pacejka [9]. Moreover, aerodynamic lift and drag on the car and the trailer bodies are included in the nonlinear yaw/plane model. However, the 4DOF-NL model does not consider the lateral load transfer due to lateral accelerations.

The derivation of the governing equations of motion for the 4DOF-NL model is conducted using Lagrange's equations. The governing equations of motion for this vehicle model is offered in [Appendix B](#). The reader is referred to [10, 11] for the detailed procedure for generating the governing equations of the nonlinear vehicle model.

Nonlinear Yaw/Roll Model with 6 DOF

The nonlinear yaw/roll model with 6 DOF (hereafter called 6 DOF-NL) is generated using the procedure proposed in [10, 11]. For the 6DOF-NL model, the motions considered are the same as those used for the 4DOF-NL with the addition of roll motions, ϕ_1 for the car body and ϕ_2 for the trailer body. Similar to the 4DOF-NL model, aerodynamic forces are taken into account in the 6DOF-NL model; the Magic Formula is introduced to model the tire/road forces. Not like the 4DOF-NL model, the 6DOF-NL model considers the lateral load transfer due to lateral accelerations.

In order to account for the roll motions of car-body and trailer-body, the roll model, shown in [Figure 2](#), is introduced in the 6DOF-NL model. [Figure 2](#) shows the body, either the car-body or trailer-body, rolling around a longitudinal axis with an angle ϕ . In [Figure 2](#), m_1 denotes the car sprung mass, m_2 the car unsprung mass, T the track between the left and

right wheels, S the distance between the right and left suspensions, h_R the vertical distance from the roll center to the road surface, and $h \cos \phi$ the vertical distance between the body CG to the roll center. With no other lateral motion of the CG, the rotation around an axis passing through the body CG results in a axle lateral motion of $h \sin \phi$. It is assumed that each axle moves laterally respect to the body CG and the lateral motion is calculated using the roll center shown in [Figure 2](#). The actual axle motion is determined by the motion of the whole vehicle that is governed by the forces applied on the system.

Similar to the 4DOF-NL model, the governing equations of motion for the 6DOF-NL model is generated using Lagrange's equations. The formulation of the governing equations is implemented using the method proposed by Anderson [10, 11].

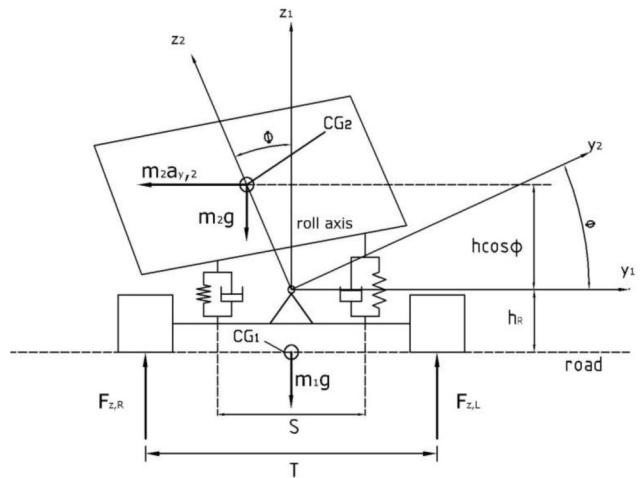


Figure 2. Roll model used in the 6DOF-NL vehicle model

Nonlinear CarSim Model with 21 DOF

In the research, a 21 DOF model based on the commercial software CarSim is generated to represent the car-trailer system. In this paper this model is called CarSim model [6]. For the towing unit, i.e., the car, the following motions are considered: the car-body is treated as a rigid body with 6 DOF; each axle is modeled as a rigid body with 2 DOF (yaw and longitudinal translation); and each car wheel has one spin DOF. Similarly, for the trailing unit, the following motions are taken into account: the trailer-body is treated as a rigid body with 6 DOF; the trailer axle is modeled as a rigid body with 2 DOF (yaw and longitudinal translation); and each trailer wheel has one spin DOF. The hitch connection between the car and the trailer results in the CarSim model with 21 DOF. The Magic Formula is used to model the tire/road forces. The geometrical parameters and configuration of the car and trailer models are illustrated in [Figure 3](#) and [Figure 4](#).

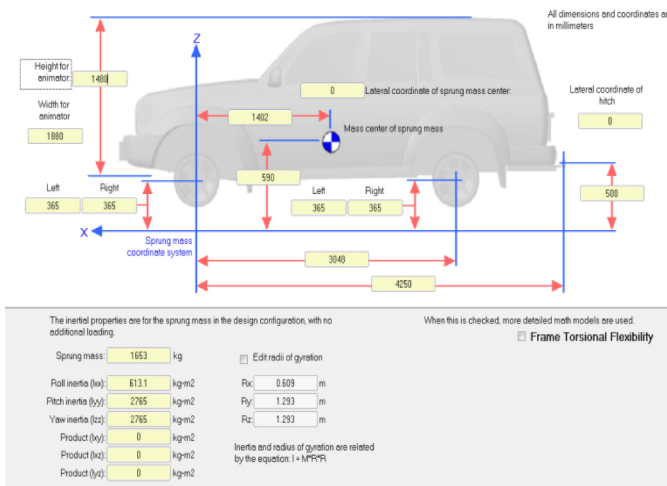


Figure 3. Geometrical parameters and configuration of the car model.

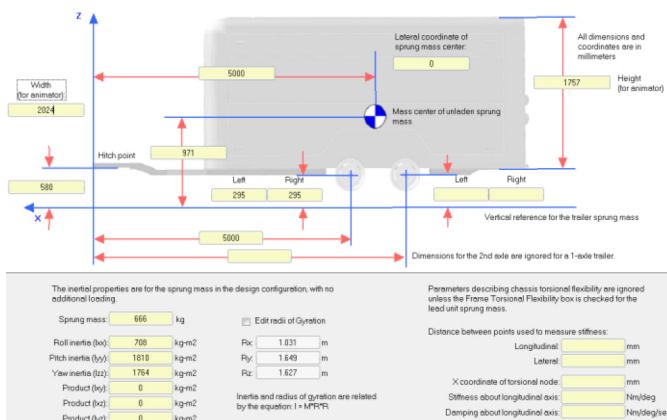


Figure 4. Geometrical parameters and configuration of the trailer model.

SIMULATION RESULTS AND DISCUSSION

In the research, the numerical simulations for the 3DOF-L, 4DOF-NL, and 6DOF-NL models are carried out using Matlab. The CarSim model is running in CarSim software. To make the simulation results obtained from different models are comparable, the aerodynamic effects in the nonlinear models are removed.

To compare the models, the following case studies are conducted: 1) an eigenvalue analysis is performed to predict the unstable motion modes of the car-trailer system using the 3DOF-L model and the result is compared with those based on the nonlinear models; 2) a single lane-change test maneuver at low lateral accelerations (less than 0.3g) is emulated; 3) a single lane-change test maneuver at high lateral accelerations (larger than 0.5g) is simulated; and 4) a Fishhook test maneuver is emulated to compare the two 3 dimensional models, i.e., the 6DOF-NL and the CarSim models.

Unstable Motion Mode Identification Based on Eigenvalue Analysis

To identify the unstable motion modes and predict the critical speed(s) of the car-trailer system, an eigenvalue analysis is conducted using the 3DOF-L model. Note that the critical speed is a vehicle forward speed above which the vehicle will lose its stability. Then, the critical speed identified using the linear model will be tested using the nonlinear models.

For the 3DOF-L model, the system matrix A can be obtained from Equation (13)

$$A = -M^{-1}D$$

(14)

With the system matrix A, the eigenvalue analysis of the model can be conducted. One pair of complex eigenvalue $S_{1,2}$ of the matrix may take the follow form

$$S_{1,2} = R_e + j\omega_d$$

(15)

where R_e and $j\omega_d$ are the real and imaginary parts of the eigenvalue. The corresponding damping ratio is defined as

$$\zeta = \frac{-R_e}{\sqrt{R_e^2 + \omega_d^2}}$$

(16)

The damping ratio is a function of vehicle forward speed. Figure 5 shows the relationship between the damping ratios (for two motion modes) and the vehicle forward speed. Curves 1 and 2 represent the damping ratios for motion modes 1 and 2, respectively. Curve 1 has the value close to 1.0, implying that the motion is well-damped and the corresponding motion mode is highly stable. For motion mode 2, once the forward speed is larger than 7 m/s, the damping ratio decreases with the speed and the ratio value approaches 0 when the speed is approximately 30 m/s. It is indicated that the critical speed is 30 m/s, above which the car-trailer system will be liable to an unstable motion mode.

To examine the critical speed based on the 3DOF-L model and identify the unstable motion mode, the dynamic responses in the time domain are presented. To excite this unstable motion mode around the critical speed (30 m/s), the car's front wheel steering angle input shown in Figure 6 is used.

The simulations based on the CarSim model show that the critical speed is approximately 35.0 m/s and the corresponding unstable motion mode is trailer swaying. Figure 7 illustrates the unstable motion mode. Figures 8, 9 and 10 illustrate simulation results in terms of the time history of the articulation angle, car lateral acceleration, and car yaw rate, respectively, using the 3DOF-L, 4DOF-NL, 6DOF-NL, and the CarSim models. When the forward speed is 30.0 m/s, the articulation angle, car lateral acceleration and car yaw rate based on the 3DOF-L, 4DOF-NL, 6DOF-NL

models increase with time and eventually the vehicle will lose stability. In contrast, at the same speed, the simulation results based on the CarSim model indicate that the car-trailer system is stable.

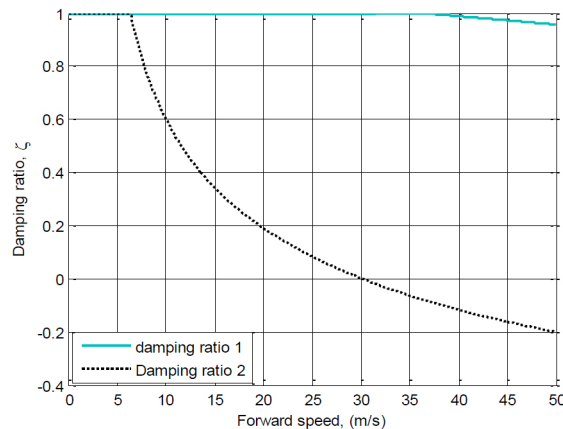


Figure 5. Damping ratios versus vehicle forward speed.

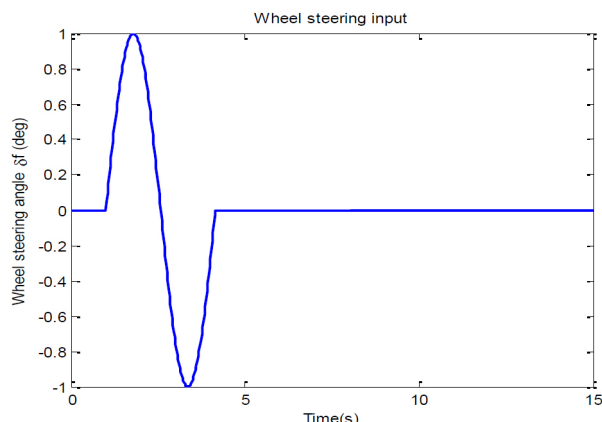


Figure 6. Car front wheel steering input for identifying the unstable motion mode

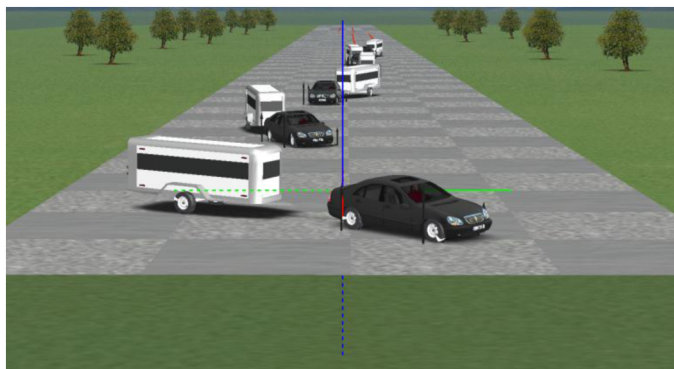


Figure 7. Visual representation of the trailer swaying motion mode at 30.6 m/s

However, once the vehicle forward speed approaches 35.0 m/s, the simulation results based on the CarSim model also

show that the articulation angle, car lateral acceleration and car yaw rate increase with time, the system will eventually lose stability, and the unstable motion mode is trailer swaying as shown in Figure 7. A close observation of Figure 9 reveals that not similar to the cases of the other models, in the case of the CarSim model, after the time instant of 12.0 second, the car lateral acceleration will not oscillate, but maintains almost a constant value (approximately 0.7g). In addition to the result shown in Figure 9, those illustrated in Figures 7, 8, and 10 demonstrate that in the case of the CarSim model, after the time instant of 12 second, the unstable motion mode will become jack-knifing due to the large articulation angle. Unfortunately, this unstable motion mode switch is not identified by the simulations based on the 3DOF-L, 4DOF-NL, and 6DOF-NL models.

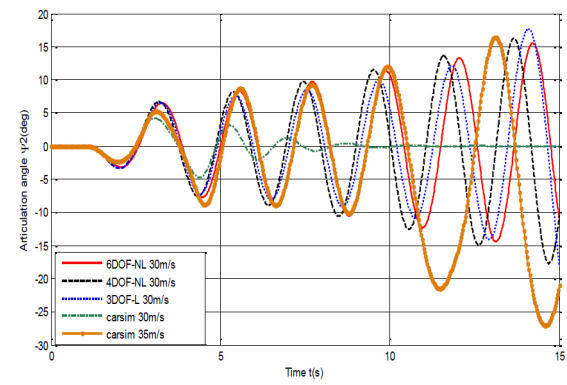


Figure 8. Articulation angle versus time

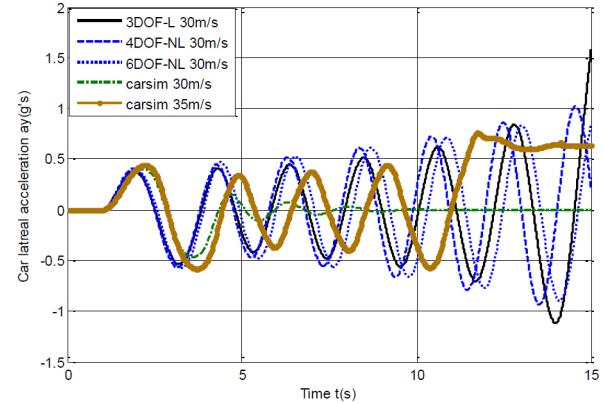


Figure 9. Car lateral acceleration versus time

The above analysis demonstrates that the simulation results in the time domain based on the 4DOF-NL, 6DOF-NL, and the carsim models match those based on the 4DOF-L model. For the linear controller design, the above eigenvalue value analysis method can also be used for critical speed(s) and unstable motion model(s) identification.

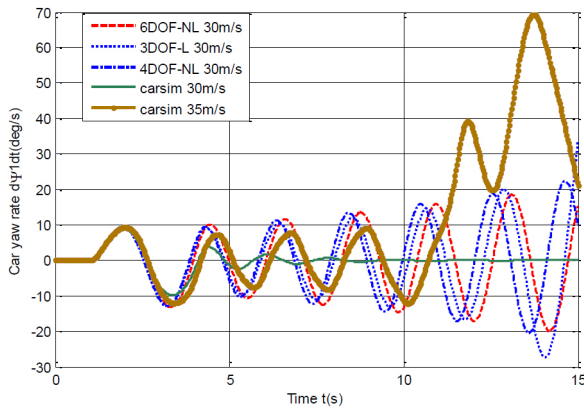
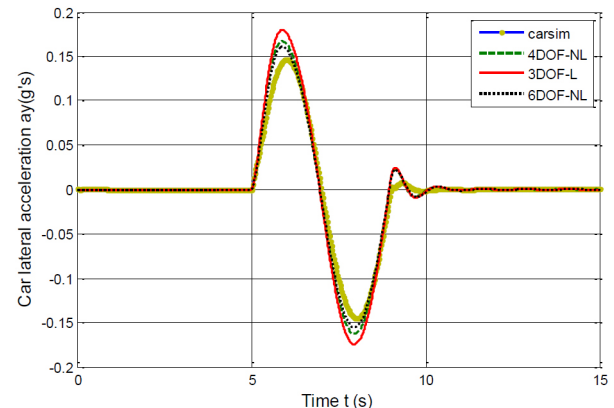


Figure 10. Car yaw rate versus time

Figure 12. Car lateral acceleration versus time under the low-g maneuver of single lane-change at $U=12.0$ m/s

Simulation Results under a Low Lateral Acceleration Maneuver

To examine the dynamic behaviors of the models in typical evasive maneuvers at low lateral accelerations (low-g), the car front wheel steering angle input shown in Figure 11 is used to simulate a single lane-change maneuver at the forward speed of 12 m/s.

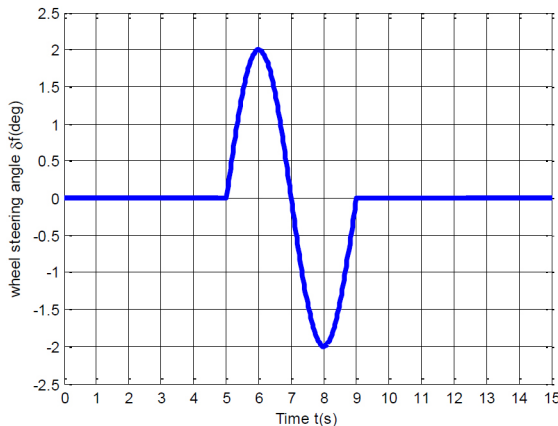
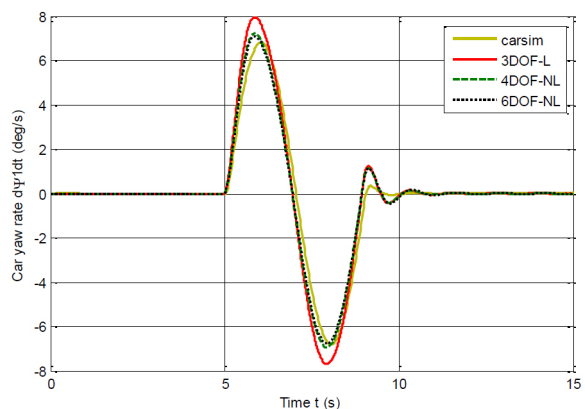
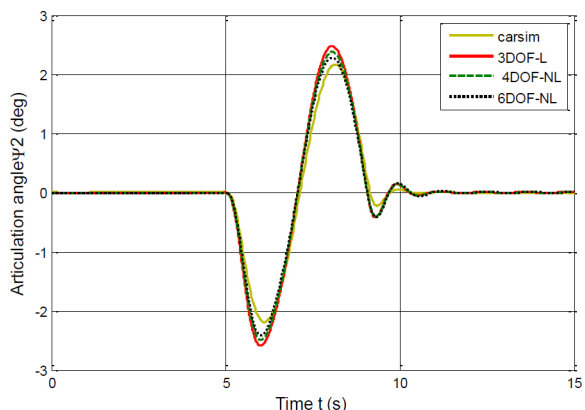


Figure 11. Car front wheel steering angle input for the single lane-change maneuver at low lateral accelerations

Figures 12, 13, and 14 show the simulation results for the low-g maneuver in terms of car lateral acceleration versus time, car yaw rate versus time, and articulation angle versus time for the models of 3DOF-L, 4DOF-NL, 6DOF-NL, and CarSim. Under the single lane-change maneuver at the forward speed of 12 m/s, the dynamic responses for all the four models are in good agreement. As shown in Figure 12, for all the cases, the car peak lateral accelerations are approximately 0.15 g. A close observation of the results shown in Figures 12, 13, and 14 disclose that for all the dynamic responses, the CarSim model achieves the least peak values and the shortest settling time, while the 3DOF-L obtains the largest peak values and longest settling time.

Figure 13. Car yaw rate versus time under the maneuver of low-g single lane-change at $U=12.0$ m/sFigure 14. Articulation angle versus time under the low-g maneuver of single lane-change at $U=12.0$ m/s

Simulation Results under a High Lateral Acceleration Maneuver

To examine the dynamic behaviors of the models under emergency evasive maneuvers at high lateral accelerations

(high-g), the car front wheel steering angle input shown in Figure 15 is used to simulate a single lane-change maneuver at the forward speed of 12.0 m/s.

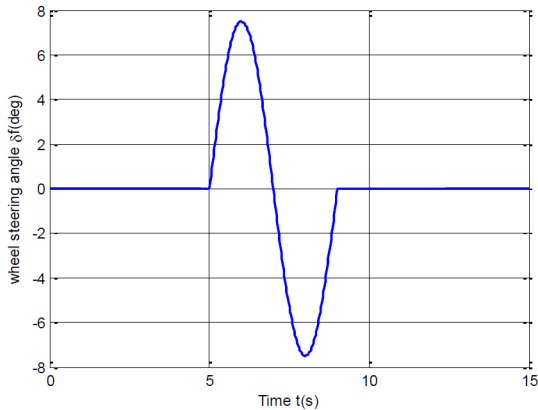


Figure 15. Car front wheel steering angle input for the high-g single lane-change maneuver

Figures 16, 17, and 18 illustrate the simulation results for the high-g maneuver in terms of car lateral acceleration versus time, car yaw rate versus time, and articulation angle versus time for the four models. Under the single lane-change maneuver at the forward speed of 12 m/s, the dynamic responses for the 4DOF-NL, 6DOF-NL and CarSim agree each other very well. As shown in Figure 16, for the three nonlinear models, the peak lateral accelerations at the CG of the car are approximately 0.55g. However, in the case of the linear model of 3DOF-L, the peak values of the car lateral acceleration, car yaw rate, and articulation angle are much larger than those of the nonlinear models. Figure 16 shows that the peak lateral acceleration reaches as large as 1.1g, which is approximately 50% larger than those of the nonlinear models.

The main reason for the huge difference of the simulation results between the linear and nonlinear vehicle models may result from the different tire models used. As expressed in Equations (7),(8),(9), the lateral tire force is a linear function of the tire side-slip angle. The lateral tire force increases with the tire side-slip angle. However, the Magic Formula specifies that once the tire side-slip angle reaches a certain value, the lateral tire force will be saturated. Simulation results shown in Figure 16 demonstrate this reasoning by the fact that the car-trailer can only achieve the peak lateral acceleration of the car at the value around 0.55g because of the lateral tire force saturation. However, without the limitation of the lateral tire force saturation, the 3DOF-L vehicle model can achieve the peak lateral acceleration of the car at the value of 1.1g, which may not be achievable in reality. Thus, it can be concluded that the linear vehicle model is not suitable for the lateral stability controller design considering emergency maneuvers at high lateral accelerations (larger than 0.5g).

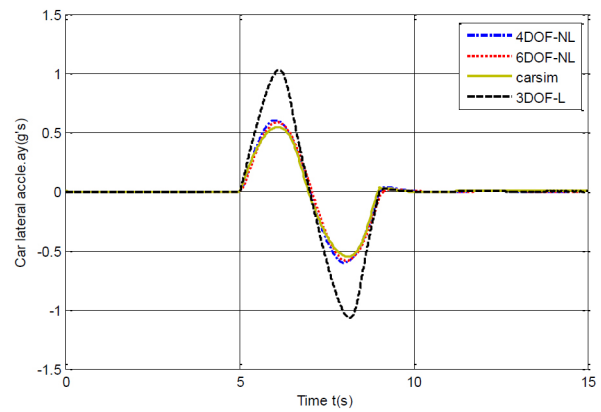


Figure 16. Car lateral acceleration versus time under the high-g maneuver of single lane-change at U=12.0 m/s

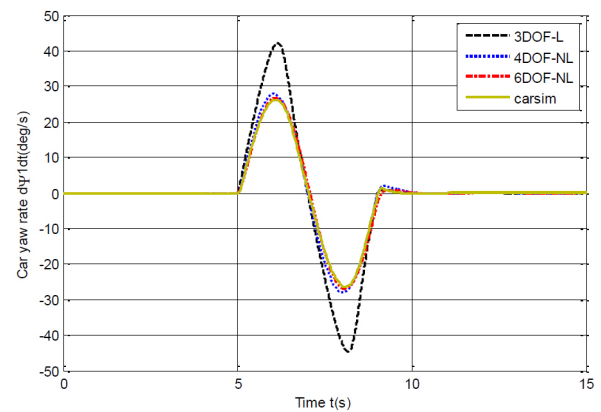


Figure 17. Car yaw rate versus time under the maneuver of high-g single lane-change at U=12.0 m/s

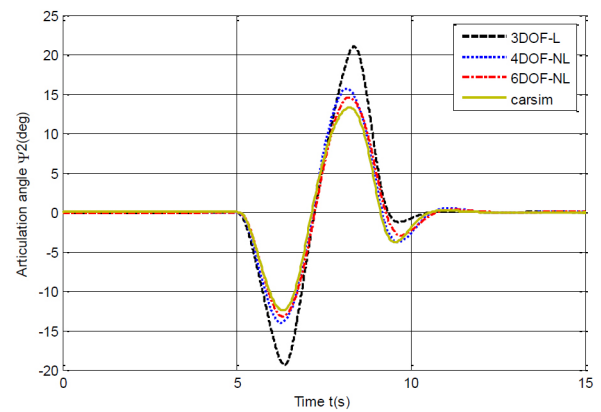


Figure 18. Articulation angle versus time under the high-g maneuver of single lane-change at U=12.0 m/s

Simulation Results under a Fishhook Testing Maneuver

To further test the effectiveness of the 6DOF-NL, the simulation results of the model under an emulated Fishhook maneuver are compared with those of the CarSim model. The Fishhook testing maneuver is designed to assess the rollover stability of road vehicles. Figure 19 shows the car steering wheel angle input for the Fishhook testing maneuver [4, 12]. In the maneuver, the vehicle forward speed is 14.0 m/s.

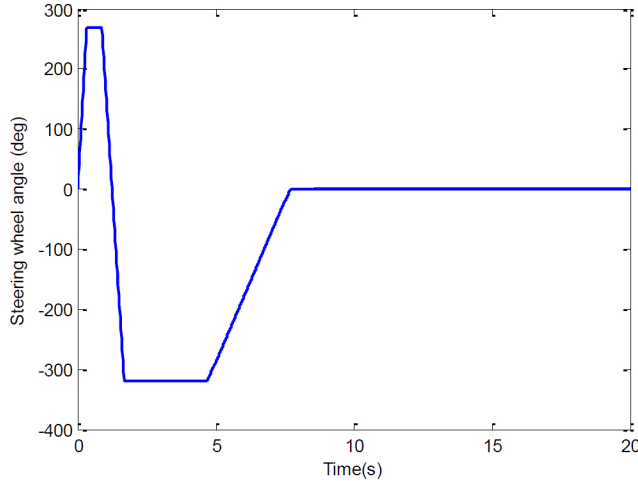


Figure 19. Steering wheel angle of fishhook steering

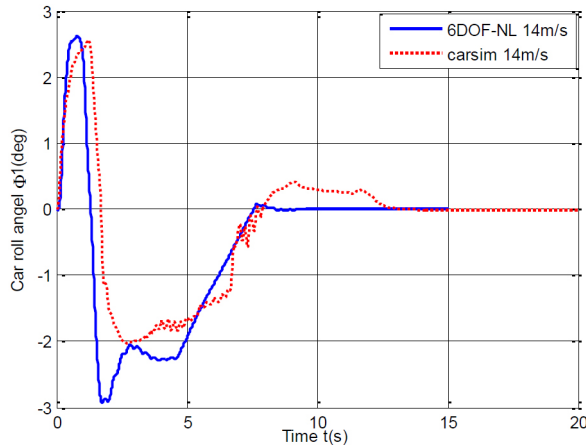


Figure 20. Car roll angle versus time under the Fishhook maneuver

Figures 20, 21, and 22 illustrate the time history of the car roll angle, car roll rate, and articulation angle for both the 6DOF-NL and CarSim models. The simulation results shows the 6DOF-NL and CarSim models agree with each in terms of car roll angle, car roll rate, and articulation angle, but with a slight difference in peak values and there are certain time delays between the corresponding peaks for the two models. The slight dynamic response differences between the two models are due to the difference of the model complexity.

Based on the above comparisons, it is believed that the 6DOF-NL model is sufficiently valid for the maneuver.

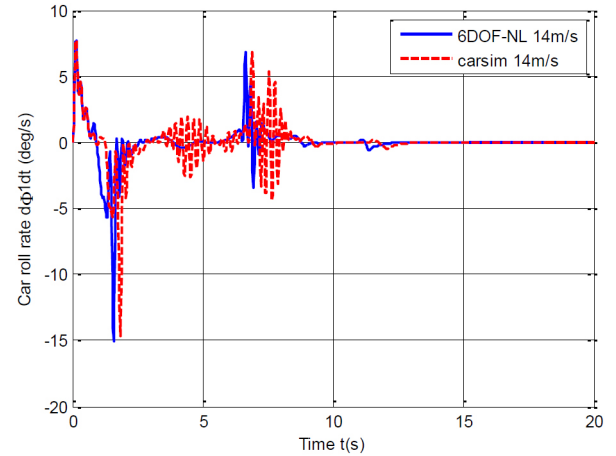


Figure 21. Car roll rate versus time under the Fishhook maneuver

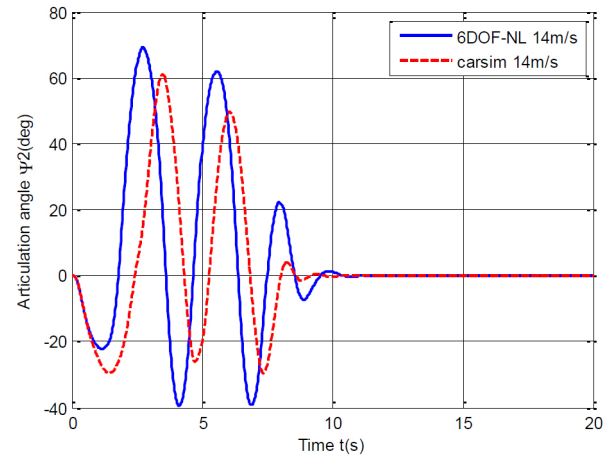


Figure 22. Car articulation angle versus time under the Fishhook maneuver

CONCLUSIONS

In this paper, three car-trailer system models are compared against the 21 degrees of freedom (DOF) model developed in CarSim commercial software in terms of fidelity, complexity, and applicability for lateral motion controller design. The linear model with 3 DOF is effective to predict the lateral stability (critical speed and unstable motion mode) of the car-trailer system. Under the regular evasive maneuvers at low lateral acceleration (less than 0.3g), this linear model can be used to provide dynamic responses that are in good agreement with the nonlinear vehicle models. Thus, this simple linear yaw/plane model can be efficiently used for the lateral motion controller design for low lateral acceleration maneuvers and without considering the roll motions of the car and trailer. However, this linear yaw/plane model is not suitable for the lateral stability controller design

for high lateral acceleration maneuvers (larger than 0.5g) and considering the roll motions of the car and trailer, because the lateral tire force saturation is not taken into account. It is demonstrated that compared with the 21 DOF model, the nonlinear yaw/rolling model with 6 DOF is effective in terms of fidelity, complexity, and computational efficiency. The 3 dimensional model with 6 DOF can be used for lateral stability controller design considering maneuvers at high lateral accelerations and accounting for roll motions of the car and the trailer. The controller performance derived from the linear 3 DOF model and the nonlinear 6 DOF model are being examined by the authors and the corresponding results will be reported in the near future.

REFERENCES

1. Clay, A., Montufar J. and Middleton D., "Operation of Long Semi-Trailers in the United States," *Transportation Research Record*, Vol. 1833, pp.79-86, 2003.
2. Shamim, R., Islam, M., and He, Y., "A Comparative Study of Active Control Strategies for Improving Lateral Stability of Car-Trailer Systems," *SAE Technical Paper 2011-01-0959*, 2011, doi: [10.4271/2011-01-0959](https://doi.org/10.4271/2011-01-0959).
3. Sharp, R.S., and Alonso Fernandez, M.A., "Car-Caravan Snaking Part 2: Active Caravan Braking," MS thesis, School of Engineering, Cranfield University, Bedford, 2001.
4. Eisele, D.D. and Peng, H., "Vehicle Dynamics Control with Rollover Prevention for Articulated Heavy Trucks," *Proceedings of 5th Int'l Symposium on Advanced Vehicle Control*, August, Ann Arbor, Michigan, pp. 22-24, 2000.
5. He, Y. and Islam, M.M., "An Automated Design Method for Active Trailer Steering Systems of Articulated Heavy Vehicles," *Transactions of ASME, Journal of Mechanical Design*, Vol. 134/041002, pp.1-15, 2012.
6. Mechanical Simulation, "CarSim Math Models," carsim.com.
7. Ellis, J.R., "Vehicle Dynamics", Business Books Limited, London, 1969.
8. Wong, J.Y., "Theory of Ground Vehicles", John Wiley & Sons, Inc., Hoboken, New Jersey, 2008.
9. Bakker, E., Nyborg, L., and Pacejka, H., "Tyre Modelling for Use in Vehicle Dynamics Studies," *SAE Technical Paper 870421*, 1987, doi: [10.4271/870421](https://doi.org/10.4271/870421).
10. Anderson, R.J., "Dynamic Handling Characteristics of Car-Trailer Systems: Development and Validation of Mathematical Models," Ph.D. Thesis, Queen's University at Kingston, Ontario, Canada, 1977.
11. Anderson, R. and Kurtz, E., "Handling-Characteristics Simulations Of Car-Trailer Systems," *SAE Technical Paper 800545*, 1980, doi: [10.4271/800545](https://doi.org/10.4271/800545).
12. Ackermann, J. and Odenthal, D., "Damping of Vehicle Roll Dynamics by Gain Scheduled Active Steering," *Proceedings of European Control Conference*, Karlsruhe, Germany, 1999.

CONTACT INFORMATION

Dr. Yuping He
 Associate Professor
 Faculty of Engineering and Applied Science
 University of Ontario Institute of Technology
 Oshawa, Ontario, Canada L1H 7K4
Yuping.he@uoit.ca

ACKNOWLEDGMENTS

This work was support by the Natural Science and Engineering Research Council of Canada (NSERC-CRDPJ 386875) and the Canadian Foundation for Innovation (CFI-18153).

APPENDIX

APPENDIX A: MATRICES FOR THE LINEAR MODEL WITH 3 DOF

$$M = \begin{bmatrix} m_1 + m_2 & -m_2(d_1 + c) & m_2c & 0 \\ -m_2d_1 & I_1 + m_2d_1(d_1 + c) & -m_2cd_1 & 0 \\ -m_2c & I_2 + m_2c(d_1 + c) & -I_2 - m_2c^2 & 0 \\ 0 & 0 & 0 & 1 \end{bmatrix},$$

$$D = \frac{1}{\mu} \times \begin{bmatrix} c_1 + c_2 + c_3 & c_1a - c_2b - c_3(d_1 + c + d_2) - (m_1 + m_2)\mu^2 & c_3(d_2 + c) & c_3\mu \\ c_1a - c_2b - c_3d & c_1a^2 + c_2b^2 + c_3d_1(d_1 + c + d_1) + m_2d_1\mu^2 & -c_3d_1d_2 & -c_3d_1\mu \\ -c_3(d_2 + c) & c_3(d_1 + c + d_2)(d_2 + c) + m_2c\mu^2 & -c_3(d_2 + c)^2 & -c_3(d_2 + c)\mu \\ 0 & 0 & \mu & 0 \end{bmatrix}$$

$$F = \begin{bmatrix} -C_f \\ -C_f a \\ 0 \\ 0 \end{bmatrix}.$$

APPENDIX B: GOVERNING EQUATIONS FOR THE NONLINEAR MODEL WITH 4 DOF

$$\begin{bmatrix} m_r + m_c & 0 & m_r d_2 \sin(\psi_2) & m_r d_2 \sin(\psi_2) \\ 0 & m_r + m_c & -m_r(d_1 + d_2 \cos(\psi_2)) & -m_r d_2 \cos(\psi_2) \\ m_r d_2 \sin(\psi_2) & -m_r(d_1 + d_2 \cos(\psi_2)) & (I_c + I_r + 2m_r d_1 d_2 \cos(\psi_2)) & I_r + m_r d_1 d_2 \cos(\psi_2) + m_r d_2^2 \\ m_r d_2 \sin(\psi_2) & -m_r d_2 \cos(\psi_2) & I_r + m_r d_1 d_2 \cos(\psi_2) + m_r d_2^2 & I_r + m_r + d_2^2 \end{bmatrix} * \begin{bmatrix} \dot{U} \\ \dot{V} \\ \dot{\psi}_1 \\ \dot{\psi}_2 \end{bmatrix}$$

$$= \begin{bmatrix} (m_r + m_c)V\dot{\psi}_1 - m_r d_1 \dot{\psi}_1^2 - m_r d_2 \cos(\psi_2)(\dot{\psi}_1 + \dot{\psi}_2)^2 + X_j \cos(\delta_j) + X_r \cos(\delta_r) + X_t \cos(\psi_2) \\ -Y_j \sin(\delta_j) - Y_r \sin(\delta_r) - Y_t \sin(\psi_2) + X_{Ac} + X_{At} \cos(\psi_2) - Y_{At} \sin(\psi_2); \\ -(m_r + m_c)U\dot{\psi}_1 - m_r d_2 \sin(\psi_2)(\dot{\psi}_1 + \dot{\psi}_2)^2 + X_j \sin(\delta_j) + X_r \sin(\delta_r) + X_t \sin(\psi_2) \\ + Y_j \cos(\delta_j) + Y_r \cos(\delta_r) + Y_t \cos(\psi_2) + Y_{Ac} + X_{At} \sin(\psi_2) + Y_{At} \cos(\psi_2); \\ m_r d_2(V \sin(\psi_2) + U \cos(\psi_2))\dot{\psi}_1 + m_r d_1 \dot{\psi}_1 + m_r d_1 d_2 \sin(\psi_2)(\dot{\psi}_2^2 + 2\dot{\psi}_1 \dot{\psi}_2) \\ + aX_j \sin(\delta_j) - bX_r \sin(\delta_r) - d_1 X_t \sin(\psi_2) + aY_j \cos(\delta_j) - bY_r \cos(\delta_r) - (d_2 + c + d_1 \cos(\psi_2))Y_t \\ - Y_{Ac} P_{Acx} - d_1 X_{At} \sin(\psi_2) - (d_2 + p_{Atx} + d_1 \cos(\psi_2))Y_{At} + T_j + T_r + T_t + T_{Ac} + T_{At}; \\ m_r d_2(V \sin(\psi_2) + U \cos(\psi_2))\dot{\psi}_1 - m_r d_1 d_2 \sin(\psi_2)\dot{\psi}_1^2 - (d_2 + c)Y_t - (d_2 + p_{Atx})Y_{At} + T_t + T_{At} - T_{yb} \end{bmatrix}$$